Connection between Second Class Currents and the $\Delta N\gamma$ Form Factors $G_M^*(q^2)$ and $G_E^*(q^2)$

Milton Dean Slaughter

Department of Physics, University of New Orleans, New Orleans, LA 70148[*]

(Dated: December 2004)

Abstract

An interesting connection between the nucleon weak axial-vector second class current form factor $g_T(q^2)$ present in the matrix element $\langle p| A^{\mu}_{\pi^+} |n\rangle$ and the $\Delta N\gamma$ form factors $G_M^*(q^2)$ and $G_E^*(q^2)$ is derived. Using a nonperturbative, relativistic sum rule approach in the infinite momentum frame, $G_M^*(q^2)$ and $G_E^*(q^2)$ are calculated in terms of $g_T(q^2)$ and the well-known nucleon isovector Sachs form factor G_M^V as input with no additional model parameters. Reasonable agreement with the data for $G_M^*(q^2)$ may be achieved with a non-zero $g_T(q^2)$ too large to be accommodated in the Standard Model. We surmise that it is plausible that second class current-associated pion cloud effects are playing a significant role in pion electroproduction processes and perhaps must be taken into account in those methodologies which utilize effective Lagrangians.

PACS numbers: 11.40.-q, 12.15.-y, 13.40.Gp, 13.60.Rj, 14.20.Gk

[*]Electronic address: E-Mail: mslaught@uno.edu

The study of the nucleon weak axial-vector second class current (SCC)[1] form factor $g_T(q^2)$ present in the matrix element $\langle p| A^\mu_{\pi^+} |n\rangle$ and the $\Delta N\gamma$ form factors $G^*_M(q^2)$ and $G^*_E(q^2)$ has engendered much experimental and theoretical research for several decades[2, 3, 4, 5, 6, 7, 8, 9, 10, 11, 12, 13, 14]. In a perfect world with unbroken $SU_F(N)$ flavor symmetry, one expects that $G^*_E(q^2) = 0$ and that $G^*_M(q^2)$ would exhibit the same q^2 behavior as does the Sachs nucleon form factor G_M. Instead, one unexpectedly finds that, experimentally, G^*_M decreases faster as a function of $Q^2 \equiv -q^2$ than does G_M and furthermore, that not only does the ratio $-G^*_E/G^*_M \neq 0$ but indeed, possesses a complicated behavior as a function of Q^2. In this Letter, we suggest that the inclusion of SCC effects normally neglected in most experimental and theoretical studies in general and in pion photoproduction and electroproduction processes in particular, may aid in our understanding of the basic underlying connecting physics principles responsible for such processes.

We begin by using a nonperturbative, relativistic sum rule approach in the infinite momentum frame where $G^*_M(q^2)$ and $G^*_E(q^2)$ are calculated in terms of $g_T(q^2)$ and the well-known nucleon isovector Sachs form factor G^V_M as input with no additional model parameters[15]. With regard to shape and data, reasonable agreement for $G^*_M(q^2)$ may be achieved with a non-zero $g_T(q^2)$ probably too large to be accommodated in the Standard Model (SM). We surmise that it is plausible that SCC-associated pion cloud effects are playing a significant role in pion photoproduction and electroproduction processes and perhaps must be taken into account in those methodologies which utilize effective Lagrangians.

The most general form for the matrix element of the weak current between the proton and the neutron is given by

$$\begin{aligned}
& (2\pi)^3 \sqrt{\frac{E_{p_1} E_{p_2}}{m m_n}} \langle P(p_2)| A^\mu_{\pi^+}(0) |N(p_1)\rangle \\
= \; & \bar{u}_P(p_2) \left[\{ g_A(\tilde{q}^2)\gamma^\mu + i g_T(\tilde{q}^2)\sigma^{\mu\nu}\tilde{q}_\nu + i g_P(\tilde{q}^2)\tilde{q}^\mu \}\gamma_5 \right] u_N(p_1). \qquad (1)
\end{aligned}$$

The 4-momentum transfer $\tilde{q}^2 = p_1 - p_2$. g_A, g_T, and g_P are the axial-vector, induced pseudotensor, and induced pseudoscalar form factors respectively. With respect to transformations under G-parity, g_A and g_P are represented by first-class currents (FCC) while g_T is represented by SCC. In the SM, a non-zero g_T can only arise due to quark mass and charge differences and thus the ratio $g_T/g_A$is thought to be very small or identically zero. In Ref.[15]—*assuming no SCC effects*—the $\Delta N\gamma$ transition form factors $G^*_M(q^2)$ and $G^*_E(q^2)$

were calculated in terms of well-known nucleon isovector Sachs form factor parametrized by $G_M^V(\tilde{q}^2) = \frac{1}{2}(\mu_p - \mu_n)G_{\text{dipole}}(\tilde{q}^2)$, with $G_{\text{dipole}}(\tilde{q}^2) \equiv [1 - \tilde{q}^2/0.71\ GeV^2/c^2]^{-2}$, where μ_p and μ_n are the proton and neutron magnetic moments respectively. On the other hand, *if one now allows for SCC effects*, one obtains:

$$G_M^*(q^2) = \left(3c_2(q^2)G_M^V(\tilde{q}_+^2) + c_1(q^2)c_3(q^2)\sqrt{\tilde{Q}_+^+\tilde{Q}_-^-}G_M^V(\tilde{q}_-^2)\right) / \left((3 + c_1(q^2))\sqrt{\tilde{Q}_+^+}\right), \quad (2)$$

$$G_E^*(q^2) = \left(c_2(q^2)G_M^V(\tilde{q}_+^2) - c_3(q^2)\sqrt{\tilde{Q}_+^+\tilde{Q}_-^-}G_M^V(\tilde{q}_-^2)\right) / \left((3 + c_1(q^2))\sqrt{\tilde{Q}_+^+}\right), \quad (3)$$

$$c_1(q^2) = \frac{m^*(4m - m^*) + m^2 - q^2}{(m^{*2} + m^2 - q^2)}, \quad (4)$$

$$c_2(q^2) = \frac{5\sqrt{3}}{3}\left[-\left(\frac{m^*m}{m^* + m}\right)\left(\frac{\tilde{Q}_+^+\sqrt{\tilde{Q}_+^-}}{(m^{*2} + m^2 - q^2)G_M^V(\tilde{q}_+^2)}\right)\left(\frac{g_T(\tilde{q}_+^2)}{g_A(0)\sqrt{4\pi\alpha}}\right) + \frac{2m^*m^2\sqrt{Q^+}}{(m^* + m)(m^{*2} + m^2 - q^2)}\right], \quad (5)$$

$$c_3(q^2) = \frac{m}{(m^* + m)\sqrt{\tilde{Q}_+^-}}, \quad (6)$$

where $\alpha \equiv$ fine-structure constant, $q \equiv p^* - p$, $p^* = (p^{*0}, \vec{t})$ and $p = (p^0, \vec{s})$ are the four-momenta of the Δ^+ and nucleon respectively, $m^* = \Delta^+$ mass, $m =$ proton mass $\approx$ neutron mass $= m_n$, $\tilde{q} = \tilde{p}^* - \tilde{p}$, $p_1 = \tilde{p}^* = (\tilde{p}^{*0}, \vec{t})$ and $p_2 = \tilde{p} = (\tilde{p}^0, \vec{s})$, $Q^\pm \equiv (m^* \pm m)^2 - q^2$, $\tilde{q}_\pm^2 = [(m^{*2} + m^2)q^2 + (m^{*2} - m^2)(\pm\sqrt{Q^+Q^-} - (m^{*2} - m^2))]/(2m^{*2})$, $\tilde{Q}_\pm^+ \equiv 4m^2 - \tilde{q}_\pm^2$, and $\tilde{Q}_\pm^- \equiv -\tilde{q}_\pm^2$. Note that $\tilde{q}_+^2(q^2 = 0) = 0$ and also that g_P does not contribute to G_M^* and G_E^* in Eqs.(2) and (3). While very little is known about g_T, it is traditional to model g_T as a dipole similar to g_A and G_M: $g_T(\tilde{q}_+^2)) = g_T(0)[1 - \tilde{q}_+^2/m_T^2]^{-2}$, where m_T is a "pseudotensor mass" analogous to the axial-vector mass $m_A \approx 1.2\,GeV/c^2$. However, we note, that at present, no theoretical justification for a specific form of g_T is known. Indeed, we find that an exponential form such as $g_T(\tilde{q}_+^2)) = g_T(0)[exp(\tilde{q}_+^2/m_T^2)]$ may also suffice. We also note that $G_M^*(q^2)$ as defined above is related to another widely used phenomenological form factor $G_M^{*Ash}(q^2)$ [16] by $G_M^*(q^2) = G_M^{*Ash}(q^2)\sqrt{1 - q^2/(m^* + m)^2}$ [5].

From Eqs. (2–6) and given a specific form for g_T, one may calculate G_M^* and G_E^*. In Fig. 1, we present our results for $G_M^{*Ash}(Q^2)$ normalized relative to $3\,G_{\text{dipole}}(Q^2)$ along with experimental data. In Fig. 2, we present our results for $G_E^*(Q^2)$ in terms of the ratio $R_{EM} \equiv -G_E^*/G_M^*$. As is evident, an adequate fit may be achieved by assuming a non-zero

g_T. Interestingly, an exponential form for g_T suffices as well as a dipole form when one considers R_{EM} and its behavior in the region $0 \leq Q^2 \lesssim 1$ $(GeV/c)^2$.

In addition to demonstrating the faster than dipole decrease in G_M^* as a function of Q^2—in agreement with experiment—and the change in sign of R_{EM} as Q^2 increases—as indicated by experiment—the curves in Fig. 1 and Fig. 2 suggest that the small (close to the real photon point) Q^2 behavior of both G_M^* and G_E^* may be much more complex than one may have perhaps anticipated and indeed may signal the presence of a SCC contribution to basic pion electroproduction processes. If this is indeed the case, a possible explanation could be pion cloud effects associated with the matrix element $\langle p| A^{\mu}_{\pi^0} |p\rangle \propto \langle p| A^{\mu}_{\pi^+} |n\rangle$ which may have to be explicitly included in dynamical approaches to pion photoproduction and electroproduction.

The author is grateful to Professor Paul Stoler for providing data used in this work and for very useful and provocative communications.

---

[1] S. Weinberg, Phys. Rev. **112**, 1375 (1958).

[2] B. Holstein, Phys. Rev. **C4**, 764 (1971).

[3] K. Kubodera, J. Delorme, and M. Rho, , Phys. Rev. Lett. **38**, 321 (1977).

[4] E. H. Monsay, Phys. Rev. **D16**, 609 (1977).

[5] H. F. Jones and M. Scadron, Ann. Phys. **81**, 1 (1973).

[6] L. A. Ahrens, *et al.*, Phys. Lett. **202B**, 284 (1988).

[7] P. Stoler, Phys. Rep. **226**, 103 (1993).

[8] H. Shiomi, Nucl. Phys. **A603**, 281 (1996).

[9] T. Minamisono *et al.*, Phys. Rev. Lett. **80**, 4132 (1998).

[10] D. H. Wilkinson, Nucl. Instrum. Meth. **A455**,656 (2000).

[11] K. Minamisono *et al.*, Nucl. Phys. **A663**, 951 (2000).

[12] S. Gardner and C. Zhang, Phys. Rev. Lett. **86**, 5666 (2001).

[13] H. Abele, *et al.*, Phys. Rev. Lett. **88**, 211801 (2001).

[14] K. S. Kuzmin, V. V. Lyubushkin, V. A. Naumov, hep-ph/0408107 (2004).

[15] M. D. Slaughter, Nuc. Phys. **A740**, 383 (2004).

[16] W. W. Ash *et al.*, Phys. Lett. **24B**, 165 (1967).

[17] S. S. Kamalov *et al.*, Phys. Rev. **C64**, 032201(R) (2001); S. S. Kamalov *et al.*, Nuc. Phys. **A684**, 321c (2001).

[18] L. M. Stuart *et al.*, Phys. Rev. **D58**, 032003 (1998).

[19] S. Stein *et al.*, Phys. Rev. **D12**, 1884 (1975).

[20] C. Mistretta *et al.*, Phys. Rev. **184**, 1487 (1969).

[21] R. Beck *et al.*, Phys. Rev. **C61**, 035204 (2000).

[22] G. Blanpied *et al.*, Phys. Rev. **C64**, 025203 (2001).

[23] V. V. Frolov *et al.*, Phys. Rev. Lett. **82**, 45 (1999).

[24] K. Joo *et al.*, Phys. Rev. Lett. **88**, 122001-1 (2002).

[25] C. Mertz *et al.*, Phys. Rev. Lett. **86**, 2963 (2001).

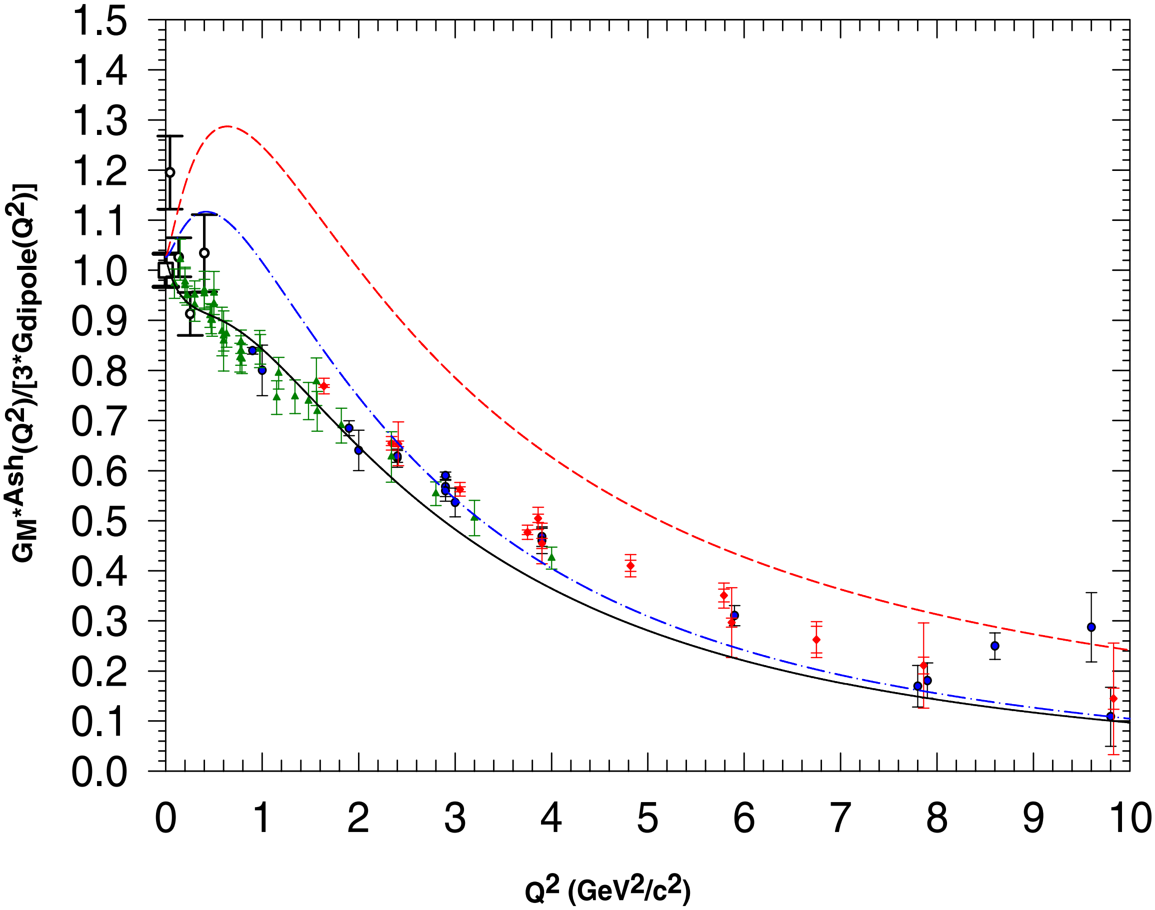

FIG. 1: $G_M^{*Ash}(Q^2)$ normalized to $3\,G_{\rm dipole}(Q^2)$. Theoretically calculated Dashed curve with $g_T = 0$ as discussed in the text with $G_M^*(0)/3\,G_{\rm dipole}(0) = 1.03$; The Solid curve is a g_T dipole fit to the JLAB G_M^* data of Ref. [17] where $g_T(0)/g_A(0) = 1.169\ c^2/GeV$, $m_T = 0.534\ GeV/c^2$ is obtained; The Dot-Dashed curve is a g_T exponential fit to the JLAB G_M^* data of Ref. [17] where $g_T(0)/g_A(0) = 0.663\ c^2/GeV$, $m_T = 0.630\ GeV/c^2$ is obtained; Open Square data point is from Ref. [16]) where $G_M^*(0) = 3.00 \pm .01$; Diamond denoted data is from Ref. [18]; Down-Triangle denoted data is from Ref. [19]; Square denoted data is from Ref. [7]; Open-Circle denoted data is from Ref. [20]; Up-Triangle denoted data is from Ref. [17].

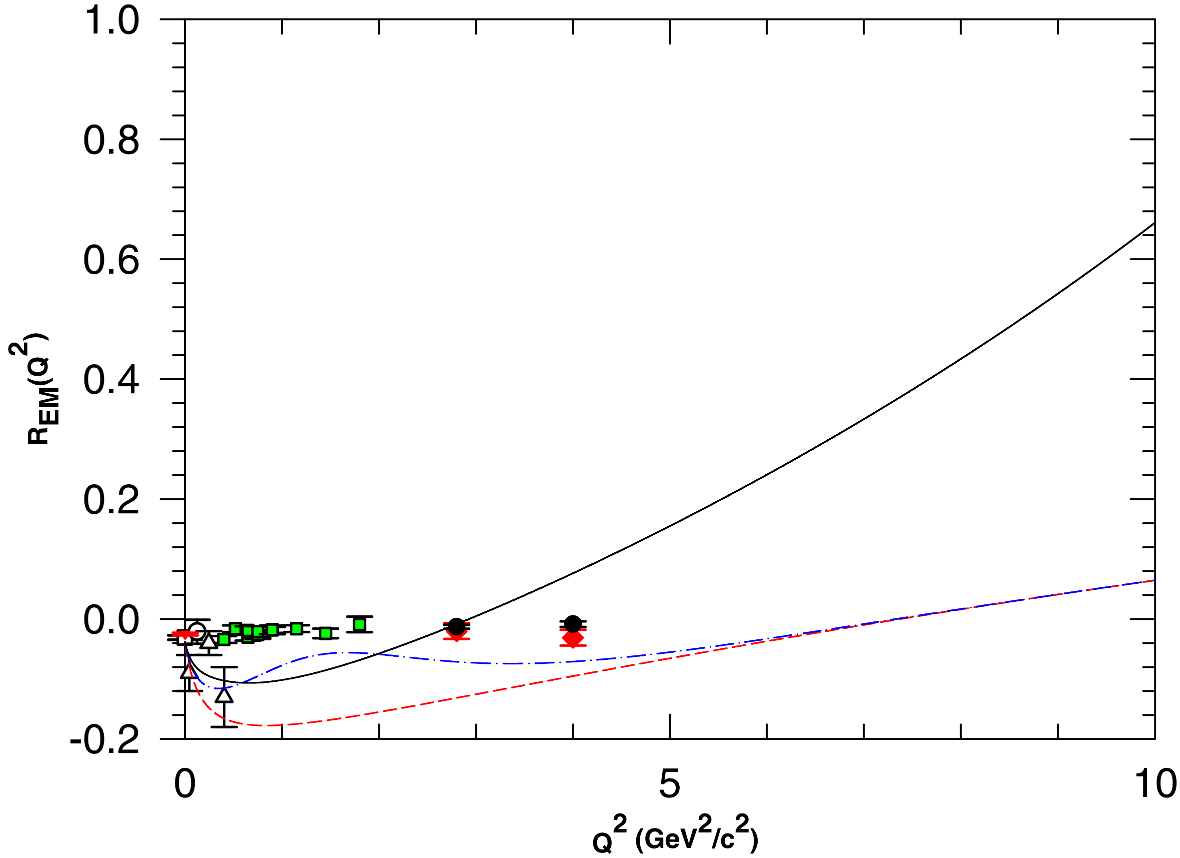

FIG. 2: Electromagnetic ratio $R_{EM}(Q^2)$. Theoretically calculated Dashed curve with $g_T = 0$ as discussed in the text with $R_{EM}(0) = -0.038$; The Solid curve utilizes the results of the g_T dipole fit to the JLAB G_M^* data of Ref. [17] where $g_T(0)/g_A(0) = 1.169\ c^2/GeV$, $m_T = 0.534\ GeV/c^2$ is obtained; The Dot-Dashed curve utilizes the results of the g_T exponential fit to the JLAB G_M^* data of Ref. [17] where $g_T(0)/g_A(0) = 0.663\ c^2/GeV$, $m_T = 0.630\ GeV/c^2$ is obtained; Open Square data point is from Ref. [22]; Diamond denoted data is from Ref. [23]; Circle denoted data is from Ref. [17]; Square denoted data is from Ref. [24]; Down-Triangle data point is from Ref. [21]; Open-Circle data point is from Ref. [25]; Up-Triangle denoted data is from Ref. [20].